Pergamon

Geochimica et Cosmochimica Acta, Vol. 61, No. 11, pp. 2167–2173, 1997

0016-7037/97 $17.00 + .00

PII S0016-7037(97)00054-9

Kinetics of the reaction $H_2O + O \Leftrightarrow 2OH$ in rhyolitic glasses upon cooling: Geospeedometry and comparison with glass transition

YOUXUE ZHANG, JULEEN JENKINS,* and ZHENGJIU XU
Department of Geological Sciences, University of Michigan, Ann Arbor, Michigan 48109-1063, USA

(*Received October* 8, 1996; *accepted in revised form January* 28, 1997)

Abstract—Controlled cooling rate experiments of hydrous rhyolitic glasses have been carried out to examine the relation between the apparent equilibrium temperature of the quenched glass (or the final quenched speciation of molecular H_2O_m and OH groups), the cooling rate, and the total H_2O content (H_2O_t). The experimental data are highly reproducible and internally consistent. Original band intensities are used to represent the data. $\bar{A}_{523}$ and $\bar{A}_{452}$ (absorbances of the 523 and 452 mm^{-1} bands in terms of peak height per mm sample thickness) are used as proxy for H_2O_m and OH, respectively. Q' ($=\bar{A}^2_{452}/\bar{A}_{523}$) is used as proxy for the equilibrium constant of the reaction. For a given cooling rate, ln Q' and ln $[\bar{A}_{523} + \bar{A}_{452}]$ are linearly related. When combined with air-quenched and water-quenched experiments reported by Silver et al. (1990), an abrupt change in slope is apparent. The experimental results provide a geospeedometer to calculate quench rates of natural hydrous rhyolitic glasses. The apparent equilibrium temperature for the reaction is roughly the same as the viscosity-defined glass transition temperature. An approximate reaction rate law for the reaction has been inferred. *Copyright © 1997 Elsevier Science Ltd*

1. INTRODUCTION

Cooling rates of rocks can be estimated on the basis of an understanding of the kinetics of homogeneous reactions inside a phase (e.g., Ganguly, 1982; Ganguly et al., 1994; Zhang, 1994; Zhang et al., 1995b). Extensive work on the interconversion reaction of hydrous species ($H_2O_m + O \Leftrightarrow 2OH$, where H_2O_m is a molecular H_2O, O is an anhydrous oxygen, and OH is a hydroxyl group associated with Si, Al, Na, etc.) in rhyolitic glasses has been carried out (Stolper, 1982a, 1982b; Zhang et al., 1991; Newman et al., 1993; Zhang et al., 1995c; Nowak and Behrens, 1995; Shen and Keppler, 1995; Ihinger et al., 1997). The reaction has recently been applied as a geospeedometer (Zhang et al., 1995c). However, the quantification of the geospeedometer (Zhang et al., 1995b) is based on experiments with only two cooling rates that are known only approximately (rapid quench at 200°C/s and slow quench at 200°C/min, Silver et al., 1990). Besides the problem associated with a limited cooling rate range, the experimental data of Silver et al. (1990) showed much scatter. It is therefore necessary to obtain data from controlled cooling rate experiments (Newman et al., 1993) to verify and revise the quantification. For example, Newman et al. (1993) discussed an experimental study in piston-cylinder apparatus in examining how the final speciation depends on cooling rates.

Another goal of our experimental study is to examine the validity of an important hypothesis. Dingwell and Webb (1990) hypothesized that the temperature of glass transition of silicate melts (T_g) as defined by viscosity is the same as the apparent equilibrium temperature (T_{ae}) of the interconversion reaction between H_2O_m and OH. (The concept of T_{ae} is similar to that of the closure temperature, T_c (Dodson, 1973). We reserve T_c to refer to the temperature at which the system becomes a closed system for kinetic processes involving diffusion and use T_{ae} to refer to the apparent equilibrium temperature of a homogeneous reaction in an open or closed system.) Dingwell and Webb (1990) applied the hypothesis to study the equilibrium of the interconversion reaction. If correct, this hypothesized equivalence might even allow accurate estimation of viscosity at very high values ($\geq 10^{12}$ Pa s) using the T_{ae} vs. cooling rate data, because the T_{ae} for the reaction can be readily determined from experiments; but such high viscosities of hydrous silicate melts are difficult to determine.

We report an experimental study on hydrous rhyolitic glasses with controlled cooling rates. The final concentrations of hydrous species after the cooling are measured. The apparent equilibrium temperature of each sample is calculated from the species concentrations. The relation between cooling rates, total water content (H_2O_t), and quenched speciation is obtained. The relation provides a geospeedometer. The data are also used to test whether $T_{ae} = T_g$, and to infer a rate law of the reaction.

2. EXPERIMENTAL AND ANALYTICAL METHODS

Controlled cooling rate experiments were conducted on natural hydrous rhyolitic glasses to examine the dependence of hydrous speciation on H_2O_t and the cooling rate. Except for the controlled cooling step, the experimental procedures generally follow those of Zhang et al. (1995b) and Wang et al. (1996), and are summarized below. A furnace was heated to a specified temperature. A glass starting sample similar to the glass chips used in Zhang et al. (1995b) was placed in the furnace and held at the temperature for a given time (typically 10 to 20 min) so that the hydrous reaction can reach equilibrium at the specified temperature. Then, the sample and furnace were cooled down at a specified cooling rate, or specified cooling method. Afterward, the sample was prepared into a doubly polished wafer. Infrared spectra of the doubly polished sample were

* *Present address:* Grand Blanc High School, 12500 Holly Rd., Grand Blanc, Michigan 48439, USA.

taken at the near infrared region with a Fourier transform infrared (FTIR) spectrometer.

Experiments were conducted in three horizontal furnaces equipped with automatic one-point temperature controllers. One furnace was equipped with an automatic cooling rate controller. Each was lined with a silica glass tube. Two thermocouples were used for each furnace: the controlling thermocouple was outside the tube and a second thermocouple was inside the tube, indicating sample temperature. During an experiment, the glass sample was next to the tip of the inside thermocouple. The inside thermocouple was calibrated against the melting point of gold or against a thermocouple so calibrated. The accuracy of the reported temperature was typically 2°C, and the reading precision was 0.1°C. However, precision, not accuracy, is important in determining the cooling rates.

Because our purpose was to examine the dependence of quenched speciation on quench rate and H_2O_t, instead of the dependence on the initial temperature (T_0), T_0 was chosen to be greater than the expected T_{ae} for the given cooling rate by ~70°C. The expected T_{ae} was estimated using Eqn. 6 of Zhang et al. (1995b). Calculations based on results in Zhang (1994) show that when $T_0 \geq T_{ae} + 50$°C, the final speciation was completely independent of T_0. If, after the experiment, the T_{ae} indicated by the final speciation was lower than T_0 by less than 50°C (due to an imperfect choice of T_0), the experiment was classified as unsuccessful and the result discarded. Ganguly (1982) and Zhang (1994) showed that the cooling rate of interest in using homogeneous reactions as geospeedometer is the cooling rate at T_{ae}, defined hereafter as q.

The experiments with slow cooling rates (0.01 to 0.3°C/min, and some experiments at 1°C/min) were carried out using the furnace with an automatic cooling rate controller. The experiments at intermediate cooling rates (1 to 3°C/min) were carried out by manually controlling the cooling rates. The manual control was achieved by repeatedly lowering the temperature of the controller by 1°C after a specified time interval. Cooling rates of ~8°C/min were achieved by turning off the furnace. Cooling rates of ~50°C/min were achieved by turning off the furnace and opening the tube furnace so that the tube was exposed to room air. In order to determine the cooling rate, the temperature of the inside thermocouple was manually recorded as a function of time (i.e., nominal cooling rates were not used).

After the cooling experiment, the glass sample was repolished to remove the thin dehydrated surface layers (except for sample 3b12-C3; see footnotes to Table 1). The final thickness for doubly-polished sections ranged from 0.33 to 3.3 mm. The sample was then analyzed by FTIR (Nicolet 60SX) for the intensities of the 523 and 452 mm^{-1} bands (for H_2O_m and OH, respectively; Stolper, 1982a). T_{ae} was determined from the quenched speciation using the calibration of Ihinger et al. (1997) (see Table 1), which is similar to that given in Zhang et al. (1991). The value of q was determined as follows. For the controlled cooling rate experiments, the T vs. t data followed a straight line, and the value of q is the absolute value of the slope of the straight line (Fig. 1a,b). For experiments cooled by turning off the furnace, the T vs. t data are nonlinear. The value of q is determined by plotting the T vs. t data and calculating the slope of the curve at $T = T_{ae}$ (Fig. 1c). The relative accuracy of q is always better than 2.6%.

Nowak and Behrens (1995) and Shen and Keppler (1995) showed that the absorbances of the 452 and 523 mm^{-1} bands change with temperature even at the temperature range of 25–300°C. They assumed that the molar absorptivities and glass thickness and density were constant and concluded that there was a portion of the reaction that could not be quenched. Since our aim is to develop a geospeedometer for volcanic glasses and to compare T_{ae} and T_g, in situ work does not serve our purpose. To examine whether the quenched speciation depends on the detailed cooling path at temperatures well below T_{ae}, we carried out two experiments (KS-C7 and KS-C8, Table 1) with different cooling histories. In experiment KS-C7, the glass was cooled at 1°C/min from 620 to 21°C. In experiment KS-C8, the glass was cooled at 1°C/min from 620 to 300°C and then quenched in liquid nitrogen. The final speciation in the two experiments agree with each other within analytical error. (The internal consistency is better than indicated by the 4.2°C difference in T_{ae} because part of the difference can be attributed to the difference in

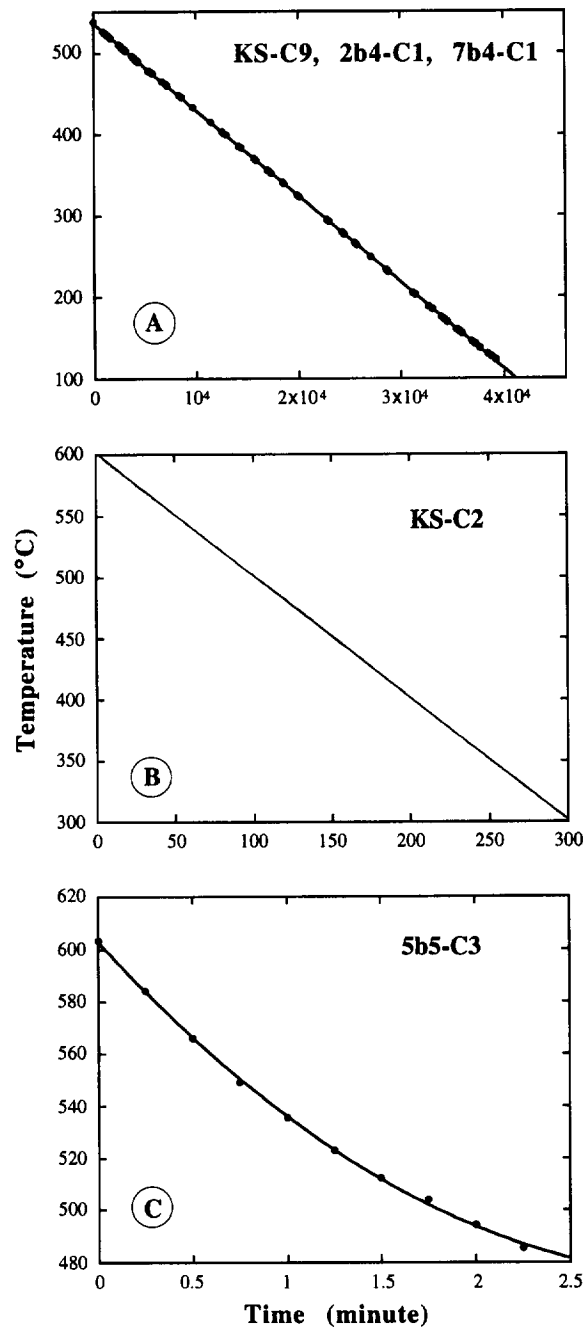

Fig. 1. Thermal history for five experiments. a. the thermal history for three experiments (running simultaneously) with automatically controlled cooling rates at 0.01°C/min (the recording is manual and not regular). b. a case for manually controlled cooling rate at 1°C/min (the 300 data points and the fitted line overlap; the symbol for the data is small because otherwise the dense data would form a wide band covering the fitted line). c. a case in which cooling is accomplished by turning off the furnace and opening the furnace. For a. b., the cooling rate is obtained from the negative slope of a straight line fit to the data. For c., the cooling rate at T_{ae} is obtained by fitting a second order polynomial to the curve as $T = m_1 + m_2(t - t_1) + m_3(t - t_1)^2$ where t_1 is chosen so that $m_1 = T_{ae}$ (for 5b5-C3, $t_1 = 1.00$ min). Not all T vs. t data are used in c. because a simple second order polynomial does not fit all data. Instead, only the data surrounding T_{ae} (roughly equal number of points for $T > T_{ae}$ and $T < T_{ae}$) are used. The cooling rate is obtained as $q = -m_2$.

Table 1. Controlled cooling rate experimental data.

Sample	q °C/min	T_0 °C	T_q °C	A_{523}	A_{452}	d mm	T_{ae} °C	H_2O_t wt%	ln Q'	q_c °C/min
KS-C9	0.0106	540	90	0.121	0.253	2.066	454	0.809%	−1.363	0.0080
2b4-C1	0.0106	479	90	0.437	0.423	2.440	398	1.571%	−1.788	0.0080
7b4-C1	0.0106	462	90	0.111	0.0685	0.330	370	2.39%	−2.049	0.0112
KS-C6	0.105	570	39	0.0879	0.196	1.526	479	0.839%	−1.247	0.126
KS-C4	0.330	600	91	0.183	0.428	3.285	492	0.839%	−1.188	0.347
7b7-C1	1.00	668	368	0.0392	0.185	1.944	568	0.513%	−0.805	1.06
KS-C7	1.07	620	21	0.166	0.421	3.205	511	0.831%	−1.100	1.24
KS-C8	1.07	620	300	0.167	0.413	3.131	506	0.840%	−1.120	1.02
KS-C2	1.00	602	300	0.0805	0.184	1.346	499	0.892%	−1.162	0.97
5b5-C1	0.99	574	274	0.0768	0.168	1.198	496	0.928%	−1.181	1.07
4b5-C1	1.01	570	270	0.294	0.390	2.190	457	1.421%	−1.444	1.39
2b3-B1	1.01	550	47	0.172	0.180	0.923	440	1.729%	−1.588	1.15
2b7-C2	1.00	550	248	0.523	0.524	2.599	436	1.824%	−1.600	1.65
3b12-C1	1.02	450	150	0.748	0.493	2.102	404	2.63%	−1.866	1.33
KS-C3	2.96	599	150	0.092*	0.257*	1.96*	531	0.811%	−1.007	3.71
3b12-C2	6.48	480	180	0.738	0.439	1.712	409	3.06%	−1.880	5.3
2b3-A1	7.49	550	65	0.120	0.143	0.719	465	1.681%	−1.434	7.9
2b7-C3	7.81	550	248	0.257	0.275	1.308	458	1.855%	−1.493	8.8
4b5-C2	8.47	570	270	0.282	0.410	2.214	484	1.433%	−1.313	9.3
5b5-C2	8.97	600	300	0.105	0.204	1.264	507	1.118%	−1.16	7.9
KS-C1	9.64	607	25	0.062*	0.185*	1.40*	549	0.802%	−0.930	9.0
3b12-C3	32.8	510	208	0.734#	0.491#	1.841#	437	3.00%	−1.723	34
4b5-C3	45.7	590	270	0.232	0.378	1.989	514	1.420%	−1.174	44
2b7-C4	49.4	550	248	0.444	0.512	2.343	482	1.879%	−1.378	39
5b5-C3	54.9	600	300	0.101	0.212	1.256	537	1.155%	−1.036	44

q: experimental quench rate at $T = T_{ae}$;
T_0: initial furnace temperature as the sample is placed into the hot spot;
T_q: the temperature at which the sample is taken out of the furnace or quenched in liquid nitrogen;
A_{523} and A_{452}: absorbances of the 523 and 452 mm^{-1} bands;
d: thickness of the doubly polished wafer;
T_{ae}: $= (2660 + 89.6\,\bar{A}_{523} + 1082\,\bar{A}_{452})/(2.482 - \ln(\bar{A}_{452}^2/\bar{A}_{523})) - 273.15$ (Ihinger et al., 1997);
H_2O_t: solved from $C(1 - C) = 0.04217\,\bar{A}_{523} + (0.04024 - 0.02011\,\bar{A}_{523} + 0.0522\,\bar{A}_{452})\,\bar{A}_{452}$ (Zhang et al., 1997);
Q': defined in Eqn. 1;
q_c: calculated cooling rate using Eqn. 3.
*: Several pieces with different thicknesses were prepared from this sample. The thickness is the average thickness and the absorbance is recalculated to correspond the average thickness.
#: The data are from one single IR spectrum without repolishing. The sample was analyzed once after the experiment without repolishing, a typical procedure, but was lost before repolishing. (For all other experiments, only data after repolishing are used though the difference in data before and after repolishing is very small.)

H_2O_t between KS-C7 and KS-C8: the glass with greater H_2O_t is quenched to a lower T_{ae}, as expected. See Fig. 2.) Therefore, detailed cooling history at low temperatures below T_{ae} has no effect on the final speciation measured at room temperature. If there is indeed a portion of the reaction that continues below T_{ae}, it would be unaffected by the cooling rate and would reach equilibrium instantaneously. Because detailed cooling history at low temperatures ($\leq$300°C) does not affect the final speciation, our approach of measuring final speciation in quenched glasses (instead of in situ measurement) for geospeedometry is valid.

3. RESULTS

We carried out 123 individual IR analyses for the twenty-five experiments. The average data of all experiments are reported in Table 1. Individual analyses (instead of averaged data) are used in figures. The maximum relative uncertainty for q (see Fig. 1) is 2.6%. Uncertainties for the thickness of glass wafers are 0.002 mm. Uncertainties for the band intensities are typically 1% relative. Because the samples may be slightly heterogeneous, the averaged data do not always reflect the very high precision in band intensities. This works to our advantage, however, because we obtained different quenched speciations for a narrow range of H_2O_t from a single sample (see 2b4-C1 in Fig. 2). T_{ae} ranges from 370 to 570°C. The cooling rate at T_{ae} ranges from 0.01 to 55°C/min. The H_2O_t ranges from 0.50 to 3.1 wt.% (Table 1). Even though H_2O_t can be accurately obtained in this concentration range based on our new calibration (Zhang et al., 1997), there are still some lingering uncertainties about the accuracy of the calibration in obtaining the species concentrations. Since knowing the actual species concentrations is not essential to the prediction of cooling rates, we will use the band intensities in presenting the results so that (1) the accuracy of the original data is not compromised by the uncertainties in determining species concentrations, and (2) no revisions to the geospeedometer will be necessary with revised calibration. We define

$$Q' = \frac{\bar{A}_{452}^2}{\bar{A}_{523}} \quad (1)$$

where $\bar{A}_{523}$ and $\bar{A}_{452}$ are, respectively, the absorbances of the 523 and 452 mm^{-1} bands (in terms of peak height) per mm

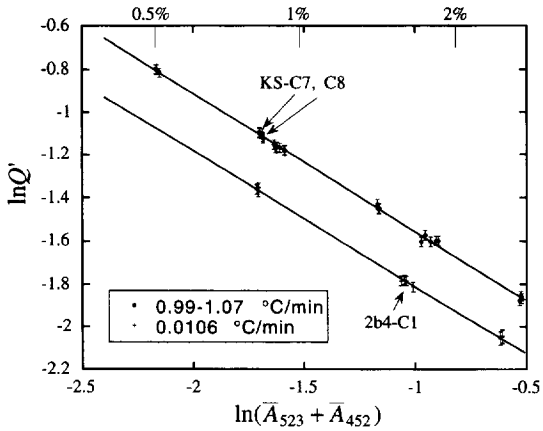

Fig. 2. ln Q' vs. ln $(\bar{A}_{523} + \bar{A}_{452})$ for two cooling rates, ~1°C/min and 0.0106°C/min. Weight percent of H_2O_t is indicated on the top x-axis. Error bars (2σ) are shown for ln Q'; error bars for ln $(\bar{A}_{523} + \bar{A}_{452})$ are smaller. The linear correlation is almost perfect. The best fit straight lines are shown as solid lines with the following equations: $y = -(2.198 \pm 0.014) - (0.643 \pm 0.009)x$ for cooling rate 0.99 – 1.07°C/min; and $y = -(2.441 \pm 0.014) - (0.630 \pm 0.011)x$ for 0.0106°C/min, where y = ln Q' and x = ln $(\bar{A}_{523} + \bar{A}_{452})$. The upper arrows point to two samples, KS-C7 and KS-C8, which show a correlation between Q' and $\bar{A}_{523} + \bar{A}_{452}$, even though the variation in H_2O_t (recall that $\bar{A}_{523} + \bar{A}_{452}$ is proxy for H_2O_t) is small. The lower arrow (2b4-C1) indicates several points in the same sample slightly heterogeneous in H_2O_t; a correlation between ln Q' and ln $(\bar{A}_{523} + \bar{A}_{452})$ exists even in this small concentration range.

sample thickness. In the above definition of Q', $\bar{A}_{523}$ and $\bar{A}_{452}$ are used as proxy for H_2O_m and OH contents, respectively. Hence, the definition of Q' is simply a variation of the Q (it would be the equilibrium constant K if equilibrium is reached) in Zhang et al. (1995b). Figure 2 shows ln Q' vs. ln $(\bar{A}_{523} + \bar{A}_{452})$ for different samples at two cooling rates (1.0 and 0.01°C/min), where $(\bar{A}_{523} + \bar{A}_{452})$ is used as proxy for H_2O_t. There is a smooth, and almost perfectly linear, correlation (first noted by P. D. Ihinger, pers. commun.) with very small scatter, demonstrating the high quality of the experimental data. Furthermore, the slopes for data at q = 0.01 and 1°C/min are similar, with very small increase of slope with q.

4. PREDICTION OF COOLING RATES

In this section we discuss empirical methods for predicting cooling rates using our experimental calibration. Inferring a reaction rate law will be discussed in a later section. As shown above, for a given cooling rate q, the quenched speciation Q' depends on both q and H_2O_t. Figure 2 shows that for a given q, the relation between ln Q' and ln $(\bar{A}_{523} + \bar{A}_{452})$ is linear. Our data also show that for a given H_2O_t, there is a rough linear relation between ln Q' and ln q, though the relation can only be roughly shown experimentally because there was no series of experiments with fixed H_2O_t.

Silver et al. (1990) reported quenched speciation of hydrous rhyolitic glasses after rapid and slow quench. The rapid-quench experiments were quenched by dropping the sample from the hot bomb into the water-filled cold bomb with an estimated quench rate of ~200°C/s. The slow-quench experiments were quenched by taking the hot bomb out of the furnace and blasting compressed air onto the bomb with an estimated quench rate of ~200°C/min. Comparison of our own data with those of Silver et al. (1990) reveals that, in a ln Q' vs. ln q plot for a given H_2O_t, there is an abrupt change in slope where our data meet with theirs. Although it may be due to experimental problems associated with the data of Silver et al. (1990), the abrupt change appears to be real, implying the complexity of this reaction in a manner consistent with the conclusions of Zhang et al. (1995c). One explanation for this is that the relation between q and T_{ae} for a given H_2O_t is not Arrhenian. Another explanation would be that there is a very rapid part of the reaction which always reached equilibrium in our more slowly cooled samples (and hence does not affect the results of our experiments, accounting for the high reproducibility), but did not reach equilibrium in the air- and water-quenched samples. Since the controlled cooling rate experiments conducted in this study cannot be extended to greater cooling rates at the present time, and since complexity emerges when comparing our data to the data of Silver et al. (1990), we present best fit models for (1) our own data only, and (2) our own data plus the data of Silver et al. (1990).

All our data can be fitted well by the following equation:

$$\ln q = 21 + 7.38 \ln (\bar{A}_{523} + \bar{A}_{452}) + 10.47 \ln Q' - 0.217 \ln q \ln Q' \quad (2)$$

where q is in K/s. The above equation is independent of the calibration of the infrared technique and can be used to solve q from measured IR band intensities. The maximum and 2σ standard deviations in calculating ln q using Eqn. 2 are 0.55 and 0.44 (0.24 and 0.19 in terms of log q), respectively. (The last term in the above equation improves the fit slightly but systematically. Refit of the data without the last term generates an expression that can reproduce ln q with maximum and 2σ standard deviations of 0.80 and 0.54.) Most of the error in calculating ln q is due to the measurement error in $\bar{A}_{523}$ and $\bar{A}_{452}$ (and hence Q'), rather than in ln q (measurement error in ln q is $\leq$0.026). For example, altering $\bar{A}_{452}$ by 1% relative (or $\bar{A}_{523}$ by 3% relative) causes calculated ln q to change by ~0.4. Since the measurement error in this study is ~1% relative in each band intensity, the reproducibility of Eqn. 2 is roughly the same as measurement reproducibility. For very low H_2O_t, the relative uncertainty in $\bar{A}_{523}$ is large, and hence the calculated q using Eqn. 2 (or any of the equations below) will have very large errors. Equation 2 involves a negative infinity for dry rhyolitic glasses (0% H_2O_t), which is not a problem because Q' is not defined for dry glasses. The above equation applies when the cooling rate is less than 1 K/s (60°C/min), but cannot be applied to the more rapidly quenched data of Silver et al. (1990).

The combined dataset turns out to be difficult to fit. After some trials, it was found that the following equation fits both datasets approximately:

$$\ln q = 10.86 + 3.79x + 5.56 \ln Q' - 0.151x \ln q - 0.281x \ln Q' \quad (3)$$

where $x = \ln (\bar{A}_{523} + \bar{A}_{452})$. The maximum and 2σ standard deviations in calculating ln q using Eqn. 3 are 0.99 and 0.56 (0.43 and 0.24 in terms of log q), respectively. That is, the maximum error in reproducing q is a factor of 2.3. The maximum and 2σ standard deviations of Eqn. 3 in reproducing our own ln q data are 0.69 and 0.44. Equations 2 and 3 can be used as a geospeedometer.

In a preliminary report, Zhang et al. (1995b) used the data of Silver et al. (1990) to construct an equation relating q, T_{ae}, and H_2O_t as a geospeedometer. They extrapolated the equation to calculate cooling rates of natural hydrous glasses. Since there is an abrupt change in the slope for data in this study and the data of Silver et al. (1990), the geospeedometer developed by Zhang et al. (1995b) needs revision, especially at low cooling rates. Equations 2 and 3 in this work supersede Eqn. 6 in Zhang et al. (1995b). Recalculated quench rates and timescales for pyroclastic glasses from site bb (data in Zhang et al., 1995b) are again similar to those of air-quench (slow-quench) samples of Silver et al. (1990). When cooling rates are calculated for obsidian glasses reported in Table 4 of Zhang et al. (1995b) using our Eqn. 3 above, they range from 3×10^{-7} to 13 K/s, as compared to 3×10^{-4} to 5.5 K/s using the preliminary calibration of Zhang et al. (1995b).

Though not necessary for geospeedometry, it is important to relate q, T_{ae}, and H_2O_t (instead of the proxies) in some applications, especially when the mechanisms and activation energy of the reaction are discussed (see later discussions). All our data (but not the data of Silver et al., 1990) can be cast into the following simple equation relating q, T_{ae}, and H_2O_t:

$$\ln q = 85.9 + 7.44 \ln (H_2O_t) - 42620/T_{ae} \quad (4)$$

where H_2O_t is mass fraction (not wt%) of H_2O_t, and the calculations of T_{ae} and H_2O_t are shown in footnotes of Table 1. Note that for internal consistency, T_{ae} and H_2O_t must be calculated as shown in footnotes of Table 1 to apply Eqn. 4. The 2σ relative uncertainties for numeric parameters in the above equation are: 85.9 ± 1.6, 7.44 ± 0.15, and 42620 ± 740. The activation energy for the interconversion between H_2O_m and OH is roughly $42620R$ = 354 kJ/mol. The maximum error in using the above equation to reproduce T_{ae} from H_2O_t and q for our own data (Table 1) is 8°C (Fig. 3a). The maximum and 2σ standard deviations in using the above equation to reproduce experimental ln q from experimental data are 0.66 and 0.46 (0.29 and 0.20 in terms of $\log_{10} q$), respectively. The above equation implies that doubling H_2O_t but maintaining the same T_{ae} requires an increase of q by a factor of 174. Zhang (1994) shows that q, T_{ae}, and the reaction timescale τ (the time required for the departure from equilibrium to decrease to 1/e times the initial departure) at T_{ae} are related by $\tau = 2RT_{ae}^2/(qE)$, where E is the activation energy (the activation energy of the backward reaction is similar to that of the forward reaction because the enthalpy of the reaction is much smaller than the activation energy). Hence, the reaction timescale τ at any T and H_2O_t can be calculated as $\tau = T^2/(21320q)$—where T is in K and q (in K/s) is from Eqn. 4 by letting $T_{ae} = T$. Reaction timescales calculated this way are in general consistent with those from isothermal experiments (Fig. 3 in Zhang et al., 1995b). However, isothermal experiments reveal the complexity of the reaction; such information cannot be obtained from cooling rate experiments. Isothermal experiments also show more scatter due to complexity in the reaction kinetics and the histories of the glasses, whereas experiments in this study are independent of the histories of the glasses because all glasses are first heated to temperatures high enough to reach equilibrium.

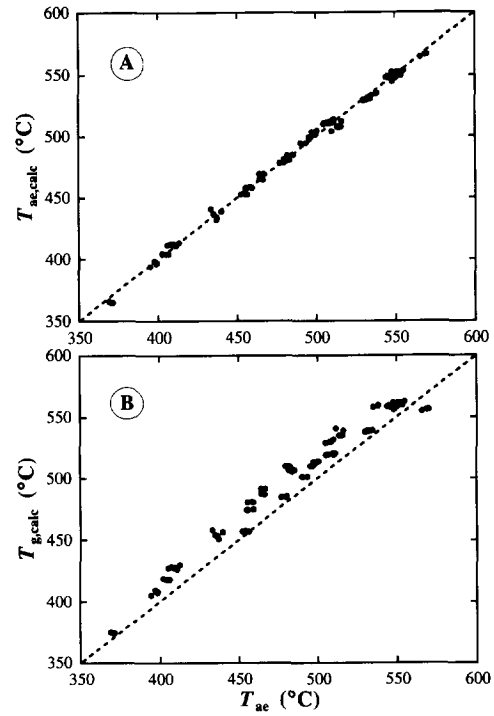

Fig. 3. a. Reproducibility of Eqn. 4 in terms of T_{ae}, i.e., a comparison of calculated T_{ae} using Eqn. 4 with experimental T_{ae} as per Ihinger et al. (1997). The dashed line is a 1:1 line. b. Comparison of calculated T_g using the viscosity model of Hess and Dingwell (1996) and experimental T_{ae}. The dashed line is a 1:1 line.

5. COMPARISON WITH GLASS TRANSITION

Our new experimental data can be used to test the validity of the hypothesis that $T_{ae} = T_g$ (Dingwell and Webb, 1990). Since one definition of rheological T_g is the temperature at which viscosity equals $10^{11.22}/q$ Pa-s where q is the cooling rate in K/s (for q = 10°C/min, T_g is the temperature at which the viscosity is 10^{12} Pa-s), T_g and T_{ae} could be compared if viscosity data are available. We have shown (Zhang et al., 1995a) that if the viscosity model of Shaw (1972) was used, T_g would be greater than T_{ae} by ~70°C. Since Dingwell and Webb (1990) calculated T_{ae} through T_g using the model of Shaw, their approach is numerically inaccurate. However, their assumption that $T_g = T_{ae}$ may still be correct, since the Shaw viscosity model has been shown to have large errors (Hess and Dingwell, 1996).

Figure 3b compares our T_{ae} data to calculated T_g using the viscosity model of Hess and Dingwell (1996). The rheologically defined T_g calculated with the Hess and Dingwell model is in good agreement with T_{ae}, and supports the assumption

of Dingwell and Webb (1990). On average, the calculated T_g is greater than T_{ae} by 13°C (Fig. 3b). This small difference may be due to uncertainties in comparing the two methods. If the difference is real, it may be explained as follows: Even though T_{ae} is uniquely defined, the definition of T_g involves some arbitrariness. For example, Stevenson et al. (1995) found that if T_g is defined as the maximum in the C_p vs. temperature curve, then T_g is the temperature at which the viscosity equals $10^{10.49}/q$ Pa-s where q is in K/s. Hence, the ~13°C difference can be attributed to the arbitrariness in the rheologically defined T_g. For example, if we define T_g to be the temperature at which viscosity equals $10^{11.6}/q$ Pa-s where q is in K/s, T_g and T_{ae} would roughly agree without a systematic difference. In other words, T_{ae} is the temperature at which the viscosity equals $10^{11.6}/q$ Pa-s (for q = 1/6 K/s = 10°C/min, T_{ae} is the temperature at which the viscosity equals $10^{12.38}$ Pa-s). Whether this relation holds depends on whether the Hess and Dingwell model can be extrapolated to lower temperatures (which depends on whether the shear modulus of rhyolitic glass changes with temperature by a factor more than 2), since their model is based on data covering a water concentration range greater than that in our T_{ae} work. Using this relation between T_{ae}, quench rate, and viscosity, one can calculate viscosity from our T_{ae} vs. q and H_2O_t data that can be used to constrain a viscosity model for hydrous rhyolitic melts, because our data provide constraints at relatively high viscosities ($10^{11.7}$ to $10^{15.4}$ Pa-s), where direct viscosity determination is difficult. Furthermore, since our data have very high precision, viscosities calculated from that data have much higher precision than the best available model (Hess and Dingwell, 1996). For example, the 2σ reproducibility of the viscosity model of Hess and Dingwell is a factor of 8.3 (2σ reproducibility is 0.92 in log η or 2.1 in ln η), whereas the 2σ reproducibility of calculated viscosity using our Eqn. 4 is a factor of 1.6 (0.46 in ln q). That is, the precision in calculated η using our data and the assumed equivalence between T_{ae} and our newly defined T_g is 5 times better than that produced by the model of Hess and Dingwell (1996).

Zhang (1994) proposed studying the glass transition using the concept of reaction kinetics. The above example shows that the idea is feasible. Henderson et al. (1996) studied the kinetics of Fe-Mn-Mg exchanges between M1 and M2 sites of olivine by neutron powder diffraction and showed that Q (quotient of the exchange reactions) vs. T curves are λ-shaped (Fig. 2 in Henderson et al., 1996), similar to typical heat capacity vs. temperature curves for glass/melt going through glass transition (Scherer, 1986). Their results further demonstrate the similarity between glass transition kinetics and chemical reaction kinetics.

6. TOWARD A REACTION RATE LAW

The almost perfect straight line in ln Q' vs. ln ($\bar{A}_{523} + \bar{A}_{452}$) (Fig. 2) implies a relation between the reaction rate coefficients and H_2O_t. Zhang et al. (1995b) have shown that the reaction rate depends strongly on H_2O_t, but the dependence was not quantified due to a lack of appropriate experimental data. In this section, we evaluate how our own data can be used to extract a rate law for the reaction:

$$H_2O_m + O \Leftrightarrow 2OH \quad (5)$$

We use a simple approach to evaluate the dependence of the reaction rate on species and H_2O_t concentrations. That is, we construct a simple reaction rate law to identify the first order effect rather than a very complicated model to account for second and third order effects. Even though Zhang et al. (1995b) have shown that the backward reaction may require diffusion of OH groups, we ignore the complexity since our experiments are not designed to examine the detailed reaction mechanisms. We write the reaction rate as:

$$d\xi/dt = k_f'[H_2O_m][O] - k_b'[OH]^2 \quad (6)$$

where ξ is the reaction progress parameter, k_f' and k_b' are the forward and backward reaction rate coefficients that may depend on H_2O_t, and brackets indicate mole fractions on a single oxygen basis (Stolper, 1982a, 1982b; Silver et al., 1990). By writing the reaction rate as Eqn. 6, we do not imply that Reaction 5 is elementary or that k_f' and k_b' are independent of H_2O_t. Any departure from the simple elementary reaction will be absorbed by the dependence of k_f' and k_b' in Eqn. 6 on H_2O_t or species concentrations (that is, k_f' and k_b' may not be the true reaction rate constants). The equilibrium constant will be referred to as K ($=k_f'/k_b'$). The expression for K is (Zhang et al., 1997)

$$K = A_K e^{-\Delta H/(RT)} \approx 6.527e^{-3110/T} \quad (7)$$

The data of Silver et al. (1990) are not used due to the apparent complexities discussed earlier. We made simplifications above because the complexities would have hampered our effort to elucidate the first order effects.

We assume that the temperature dependence of the reaction rate coefficients follows the Arrhenius relation:

$$k_f' = A_{kf} e^{-E_f/(RT)} \quad (8a)$$

$$k_b' = A_{kb} e^{-E_b/(RT)} = (A_{kf}/A_K) e^{(\Delta H - E_f)/(RT)} \quad (8b)$$

where A_{kf} and A_{kb} are the pre-exponential coefficients and may depend on H_2O_t or species concentrations, and E_f and E_b are the activation energies for the forward and backward reactions. The activation energy of the reaction, E_f, is $42620R$ = 354 kJ/mol, roughly independent of H_2O_t based on Eqn. 4. Using this activation energy, the program of Zhang (1994) is used to solve A_{kf} for each experiment so that the calculated T_{ae} after cooling at the specified q matches the experimental T_{ae}. Figure 4 shows the excellent correlation between ln A_{kf} and ln [H_2O_t]. A_{kf} is proportional to the ~7th power of H_2O_t! That is, doubling H_2O_t increases A_{kf} by a factor of 128! The expression for k_f' is hence

$$k_f' \approx 1.01 \times 10^{33}[H_2O_t]^7 e^{-42620/T}\ s^{-1} \quad (9)$$

The backward reaction rate coefficient, k_b', can be found by k_f/K. The rate law for the reaction can be written as

$$d\xi/dt = k_f[H_2O_t]^7[H_2O_m][O] - k_b[H_2O_t]^7[OH]^2 \quad (10)$$

where k_f ($=1.01 \times 10^{33}e^{-42620/T}\ s^{-1}$) and k_b ($=1.547 \times 10^{32}e^{-39510/T}\ s^{-1}$) depend on temperature but not on species or H_2O_t contents. This expression can reproduce experimental T_{ae} of our experiments with an error of ≤5°C. The

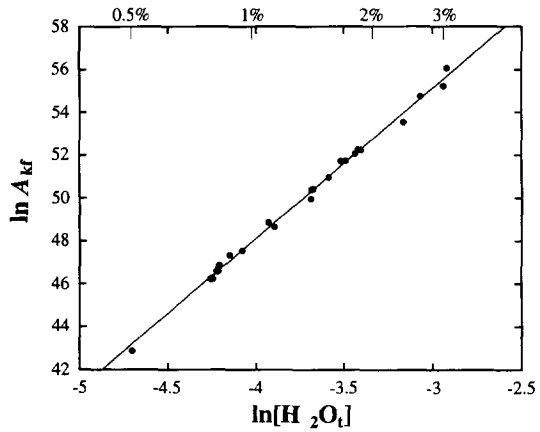

Fig. 4. ln A_{kf} vs. ln [H_2O_t], where A_{kf} is in s^{-1} and [H_2O_t] is the mole fraction of H_2O_t on a single oxygen basis. Only average data reported in Table 1 (rather than the 123 original data points) are used, because solving for A_{kf} by trial and error method is time-consuming. [H_2O_t] is calculated using $C/(0.554478 + 0.445522C)$, where C is the mass fraction of H_2O_t. The best fit line has a slope of 7.05 ± 0.19 (2σ). Hence, the data were refit by fixing the slope at 7. The line shown is the refit line. The equation of the refit is: ln A_{kf} = 76.00(±0.09) + 7 ln [H_2O_t].

high reproducibility confirms that our simple approach captures the first order effects of the kinetics of this reaction. However, the above reaction rate law still cannot be applied to the data of Silver et al. (1990).

The inferred strong dependence of the rate coefficients with H_2O_t will place a constraint on future mechanisms proposed for Reaction 5. The determination of the reaction mechanism will elucidate the reaction on the molecular, atomic, or ionic scale. Future work will involve accurate calibration so that species concentrations can be obtained from the room-temperature IR measurements and in situ high temperature measurements; more detailed experiments at constant temperature combined with in situ measurement of species concentrations at the experimental temperature; and the elucidation of a reaction mechanism that incorporates both the cooling rate data and the isothermal experimental data.

Acknowledgments—We thank D. B. Dingwell, P. D. Ihinger, and an anonymous reviewer for constructive reviews and P. Richet, J. Tangeman, and R. A. Lange for help and discussions. This research is funded by NSF grants EAR-9315918 and EAR-9458368. J. J. was partially supported by the NSF REU supplement.

REFERENCES

Dingwell D. B. and Webb S. L. (1990) Relaxation in silicate melts. *Eur. J. Mineral.* **2,** 427–449.

Dingwell D. B., Romano C., and Hess K. U. (1995) The effect of minor water contents on the viscosity of a granitic melt under P-T-X conditions relevant to silicic volcanism. *Eos* **76,** F646. abstr.

Dodson M. H. (1973) Closure temperature in cooling geochronological and petrological systems. *Contrib. Mineral. Petrol.* **40,** 259–274.

Ganguly J. (1982) Mg-Fe order-disorder in ferromagnesian silicates II: thermodynamics, kinetics and geological applications. In *Advances in Physical Geochemistry,* Vol. 2. (ed. S. K. Saxena), pp. 58–99. Springer-Verlag.

Ganguly J., Yang H., and Ghose S. (1994) Thermal history of mesosiderites: Quantitative constraints from compositional zoning and Fe-Mg ordering in orthopyroxenes. *Geochim. Cosmochim. Acta* **58,** 2711–2723.

Henderson C. M. B., Knight K. S., Redfern S. A. T., and Wood B. J. (1996) High-temperature study of octahedral cation exchange in olivine by neutron powder diffraction. *Science* **271,** 1713–1715.

Hess K. U., and Dingwell D. B. (1996) Viscosities of hydrous leucogranitic melts: A non-Arrhenian model. *Amer. Mineral.* **81,** 1297–1300.

Ihinger P. D., Zhang Y., and Stolper E. M. (1997) Speciation of water in rhyolitic glasses. (in revision).

Newman S., Blouke K., Bashir N., Ihinger P., and Stolper E. (1993) Cooling of rhyolitic volcanics-evidence from melt inclusions. *GSA Abstracts with Programs* **25,** A-43.

Nowak M. and Behrens H. (1995) The speciation of water in haplogranitic glasses and melts determined by in situ near infrared spectroscopy. *Geochim. Cosmochim. Acta* **59,** 3445–3450.

Scherer G. W. (1986) *Relaxation in Glass and Composites.* J. Wiley & Sons.

Shaw H. R. (1972) Viscosities of magmatic silicate liquids: An empirical method of prediction. *Amer. J. Sci.* **272,** 870–893.

Shen A. and Keppler H. (1995) Infrared spectroscopy of hydrous silicate melts to 1000°C and 10 kbar: Direct observation of H_2O speciation in a diamond-anvil cell. *Amer. Mineral.* **80,** 1335–1338.

Silver L., Ihinger P. D., and Stolper E. (1990) The influence of bulk composition on the speciation of water in silicate glasses. *Contrib. Mineral. Petrol.* **104,** 142–162.

Stevenson R. J., Dingwell D. B., Webb S. L., and Bagdassarov N. S. (1995) The equivalence of enthalpy and shear stress relaxation in rhyolitic obsidians and quantification of the liquid-glass transition in volcanic processes. *J. Volcanol. Geotherm. Res.* **68,** 297–306.

Stolper E. (1982a) The speciation of water in silicate melts. *Geochim. Cosmochim. Acta* **46,** 2609–2620.

Stolper E. M. (1982b) Water in silicate glasses: An infrared spectroscopic study. *Contrib. Mineral. Petrol.* **81,** 1–17.

Wang L., Zhang Y., and Essene E. J. (1996) Diffusion of the hydrous component in pyrope. *Amer. Mineral.* **81,** 706–718.

Zhang Y. (1994) Reaction kinetics, geospeedometry, and relaxation theory. *Earth Planet. Sci. Lett.* **122,** 373–391.

Zhang Y., Stolper E. M., and Wasserburg G. J. (1991) Diffusion of water in rhyolitic glasses. *Geochim. Cosmochim. Acta* **55,** 441–456.

Zhang Y., Jenkins J., Xu Z., and Belcher R. (1995a) Reaction kinetics and relaxation in silicate melts/glasses. *Eos* **76,** F646–647. abstr.

Zhang Y., Stolper E. M., and Ihinger P. D. (1995b) Kinetics of reaction $H_2O + O = 2OH$ in rhyolitic glasses: Preliminary results. *Amer. Mineral.* **80,** 593–612.

Zhang Y., Belcher R., Ihinger P. D., Wang L., Xu Z., and Newman S. (1997) New calibration of infrared measurement of water in rhyolitic glasses. *Geochim. Cosmochim. Acta* **61,** (in press).